Title

Accuracy of flat panel detector CT with integrated navigational software with and without MR fusion for single-pass needle placement

Journal

Journal of NeuroInterventional Surgery, 8(7)

ISSN

1759-8478

Authors

Mabray, Marc C
Datta, Sanjit
Lillaney, Prasheel V
et al.

Publication Date

2016-07-01

DOI

10.1136/neurintsurg-2015-011799

Peer reviewed

Published in final edited form as:

J Neurointerv Surg. 2016 July ; 8(7): 731–735. doi:10.1136/neurintsurg-2015-011799.

Accuracy of Flat Panel Detector CT with Integrated Navigational Software with and without MR Fusion for Single-Pass Needle Placement

Marc C. Mabray, MD[1], **Sanjit Datta, MS**[3], **Prasheel V. Lillaney, PhD**[1], **Teri Moore, BS**[3], **Sonja Gehrisch, MS**[3], **Jason F. Talbott, MD, PhD**[1], **Michael R. Levitt, MD**[4], **Basavaraj V. Ghodke, MD**[4,5], **Paul S. Larson, MD**[2], and **Daniel L. Cooke, MD**[1]

[1]Department of Radiology and Biomedical Imaging, University of California San Francisco, San Francisco, CA, USA

[2]Department of Neurological Surgery, University of California San Francisco, San Francisco, CA, USA

[3]Siemens Healthcare AG, Forchheim, Germany

[4]Department of Neurological Surgery, University of Washington, Seattle, WA, USA

[5]Department of Radiology, University of Washington, Seattle, WA, USA

Abstract

Purpose—Fluoroscopic systems in modern interventional suites have the ability to perform flat panel detector CT (FDCT) with navigational guidance. Fusion with MR allows navigational guidance towards FDCT occult targets. We aim to evaluate the accuracy of this system using single-pass needle placement in a deep brain stimulation (DBS) phantom.

Materials and Methods—MR was performed on a head phantom with DBS lead targets. The head phantom was placed into fixation and FDCT was performed. FDCT and MR data sets were automatically fused using the integrated guidance system (iGuide, Siemens). A DBS target was selected on the MR data set. A 10cm, 19G needle was advanced by hand in a single pass using laser crosshair guidance. Radial error was visually assessed against measurement markers on the target and by a second FDCT. 10 needles were placed using CT-MR fusion and 10 needles were placed without MR fusion, targeting based solely off of the FDCT, with fusion steps repeated for every pass.

Corresponding author: Marc C. Mabray MD, 505 Parnassus Ave M-391, San Francisco, CA 94143, Fax: 415-476-0616, Phone: 415-476-8358, marc.mabray@ucsf.edu.

Competing Interests Statement:
Three investigators (SD, TM, SG) are employees of Siemens AG. This was a collaborative project with these three authors.

Contributorship Statement:
All authors contributed to the research and to this manuscript. Specific contributions: Planning and Study Design: MCM, SD, PVL, TM, SG, JFT, MRL, BVG, PSL, DLC. Data Collection and Analysis: MCM, SD, PVL, TM, SG, JFT, PSL, DLC. Writing Manuscript: MCM, SD, PVL, TM, SG, JFT, MRL, BVG, PSL, DLC. Editing Manuscript: MCM, SD, PVL, TM, SG, JFT, MRL, BVG, PSL, DLC.

Data Sharing:
All data of interest is included in the manuscript.

Results—Mean radial error was 2.75±1.39 mm as defined by visual assessment to the center of the DBS target and 2.80±1.43 mm as defined by FDCT to the center of the selected target point. There were no statistically significant differences in error between MR fusion and non-MR guided series.

Conclusions—Single pass needle placement in a DBS phantom using FDCT guidance is associated with a radial error of approximately 2.5–3.0 mm at a depth of approximately 80 mm. This system could accurately target sub-centimeter intracranial lesions defined on MR.

Keywords

Cone-Beam Computed Tomography; Interventional Radiology; Deep Brain Stimulation; Stereotactic Techniques; Neurosurgery

INTRODUCTION

Fluoroscopic systems in modern interventional suites have the ability to perform high-quality flat panel detector cone beam computed tomography (FDCT) for diagnostic and interventional purposes.[1–12] Integrated navigational software can be used to plan a needle trajectory and provide real-time guidance for percutaneous procedures throughout the body including for intracranial, spinal, and head and neck procedures.[1–378101113–15] FDCT allows the performance of complex percutaneous procedures with the safety and convenience of performing these procedures in an interventional suite or hybrid operating room as opposed to a standard computed tomography (CT) suite.[1–38101115] FDCT data acquired at the time of or during a procedure can additionally be fused with pre-procedure magnetic resonance imaging (MRI) data to allow navigational guidance towards FDCT occult targets.[216]

Neuronavigational software for intracranial use is well established in the field of minimally invasive neurosurgery, predominantly involving navigation towards targets defined on pre-procedure MRI.[17–23] While there is some shift of intracranial contents compared to pre-procedure MRI, frameless and framed stereotactic navigational systems are highly accurate with positional errors in the range of 0.5 to 5 mm.[17–23] Deep brain stimulation (DBS) lead placement in Parkinson's disease patients requires highly accurate placement of wires into the subthalamic nucleus and is performed with real time interventional MRI guidance.[2425] Current interventional MRI navigational systems are associated with sub-millimeter positional errors at depths of 8–9 cm.[2425]

In this study we aim to assess the accuracy of single-pass needle placement with FDCT-guided navigation using two different techniques that would be applicable in two different situations. The first, using fusion with a pre-procedural MRI and MRI based targeting, simulates the performance of FDCT-guidance to a lesion visible only on MRI. The second, without pre-procedural MRI and with FDCT based targeting, simulates the performance of FDCT-guidance to a lesion visible on CT. We have chosen to measure accuracy of these techniques in simulated DBS lead placement, a procedure that requires highly accurate placement of wires into the subthalamic nucleus at a depth of 8–9 cm and is performed with real time interventional MRI guidance.[2425] This difficult task will test the limits of FDCT-guidance although the results may be applicable to different intracranial, spinal, and head

and neck procedures that could be performed with these techniques. Our hypothesis is that FDCT-guided navigation will have a radial error of less than 5mm for single-pass needle placement in a DBS phantom with and without pre-procedural MRI fusion and MRI guided targeting.

MATERIALS AND METHODS

Head phantom

An established gelatin filled head phantom with deep brain stimulation lead targets and with pre-drilled frontal burr holes was used for this study.[2425] The head phantom had 8 DBS lead targets, 4 on each side, accessible by either the right or left frontal burr hole. Each target was 10 mm in diameter and had an inner 3 mm diameter notch. The target was marked with 1mm concentric rings that were visible through a large posterior hole in the phantom to allow visual assessment of radial error.

Pre-procedure MRI

For MRI fusion guidance experiments the head phantom was imaged on the day of the experiments with a clinical DBS lead pre-procedural MRI protocol at 3 Tesla. This included a volumetric T2 weighted inversion recovery sequence (TE 45 ms, TR 3000 ms, slice thickness 2 mm, no gap) and a volumetric T1 weighted magnetization prepared rapid acquisition gradient recalled echo (MPRAGE) sequence (TE 4.5 ms, TR 1800 ms, slice thickness 1 mm, no gap). For the FDCT only experiments this step was skipped.

Preparation and targeting

The head phantom was then placed in 3-point rigid fixation with a carbon fiber Mayfield skull clamp (Mayfield Modified Skull Clamp, Integra, Plainsboro, NJ, USA), which was attached to the procedure table in the interventional angiographic suite (Artis zee biplane, Siemens, Forchheim, Germany). An 8 second FDCT was then performed (*syngo* DynaCT, Siemens, Forchheim, Germany). The FDCT and the T2 MRI data sets were then automatically fused using the FDCT integrated guidance system (*syngo* iGuide, Siemens, Forchheim, Germany). No manual adjustment was performed. The FDCT and fusion steps were repeated for every needle pass in order to include any inaccuracy introduced by the FDCT and fusion steps. The MRI fusion step was skipped for the FDCT only experiments.

For the MRI experiments a DBS target was selected within the guidance software when windowed to the MRI data set to simulate guidance to an FDCT occult lesion (Figure 1). An entry site was then selected when windowed to the FDCT data set in order to visualize the pre-drilled burr hole entry site, our necessary entry site. For the FDCT only experiments both the target and entry site were selected on the FDCT data set to simulate guidance to an FDCT visible lesion. The depth from entry site to target was recorded.

Targets were confirmed and the flat panel detector was automatically moved to the correct in-line or “bull’s-eye” projection. The positioning was checked using the maximum fluoroscopic magnification setting (11 cm field of view), and without fluoroscopic

assistance, the table was manually shimmed to line up the projected target and entry site (Figure 2).

Single pass needle placement

A piece of tape was placed over the hub of a 10 cm, 19-gauge (1.067 mm outer diameter) needle (Chiba, Cook Medical, Bloomington, IN, USA) and a crosshair was manually drawn on the tape for alignment with the system's laser crosshairs. The laser crosshairs were activated and the needle tip was positioned on the burr hole at the laser crosshair. The needle hub was aligned with the system's laser crosshair and the needle was advanced in a single pass until the target was reached (Figure 2). The operator could not see the target during the procedure. Over 3 sessions, 10 needles were placed with MRI fusion and MRI based target selection and 10 needles were placed without MRI fusion and with FDCT based target selection.

Assessment of accuracy

We visually assessed accuracy by noting the location of the needle tip on the target against the measurement markers (Figure 3). This allowed measurement of the radial error as defined to the center point of the target. A second FDCT (Figure 2) was then performed and the radial error was measured from the center of the planned target to the actual needle position. The needle was then removed. We focused on 2-dimensional radial error as our summary of targeting accuracy, as depth error measurements would be artificial due to the operator being able to feel the needle hit the target plate.

Radiation output

The air kerma and dose area product (DAP) from the entire study and from each individual step (the first FDCT, fluoroscopy, and second FDCT) were recorded upon completion.

Statistical analysis

The mean and standard deviations were calculated for target depth, visual radial error to the center of the target, visual radial error to the 3 mm notch, radial error by FDCT to the planned target, and the radiation dose metrics. The measurement results were then separated between the two groups and tested with two-tailed Mann-Whitney tests. A two-tailed p value of <0.05 would be considered statistically significant.

RESULTS

Accuracy results are presented in Table 1. The mean depth was 83.12 mm and the mean radial error was 2.75±1.39 mm (±standard deviation) as defined by visual assessment to the center of the DBS target and 2.80±1.43 mm as defined by FDCT to the center of the selected target point. There were no statistically significant differences in error or depth measurements between the experiments using MRI fusion and targeting based off of MRI and the experiments without MRI fusion and targeting based off of FDCT.

Radiation output measurements are also presented in Table 1. Mean total air kerma was 122.19 mGy and mean total DAP was 3272 uGy-m^2. The operator was only in the room for

a mean fluoroscopy time of 0.16 min with an air kerma of 1.21 and DAP of 17.28. In practice the second FDCT that was used to measure the error could possibly be omitted.

DISCUSSION

In this study we have shown that single pass needle placement in a DBS phantom using FDCT guidance in the interventional suite is associated with a radial error of approximately 2.5–3.0 mm at a depth of approximately 80 mm. We performed these experiments with fusion to a pre-procedural MRI and targeting based off of MRI and also without pre-procedural MRI with targeting based only off of FDCT. Similar error measurements were found for both sets of experiments with no statistically significant differences detected. Radiation to the patient and operator were within expected and acceptable ranges with the operator only in the room for a small amount of fluoroscopy. This system could be used with or without MRI fusion to accurately target sub-centimeter intracranial lesions and provide guidance for spinal and head and neck procedures in the interventional angiographic suite or a hybrid operating room.

The protocols that we followed in this study could potentially be applied to targeting lesions only visible on MRI if performed with fusion to a pre-procedural MRI or could be more rapidly applied to targeting a lesion visible on CT without the need for pre-procedural imaging. A third potential lower radiation dose protocol whereby a pre-procedure MRI is registered to live, 2D fluoroscopy only, without the need of FDCT, is technically possible but was not evaluated in this study. The errors that we experienced in this study are larger than the sub-millimeter errors reported with current interventional MRI technology used for DBS placement.[24,25] Accuracy assessment in our study was largely performed in a DBS phantom as a difficult procedural test that may exceed the accuracy requirements of most interventional procedures. Our positional error of 2.5–3.0 mm was within the range of positional errors reported for neurosurgical stereotactic systems, which are generally in the range of 0.5–5 mm.[17–23] A notable difference between the techniques that we used in this study and most stereotactic systems used for neurosurgical intracranial access are that we passed the needle freehand without any additional stabilization of the needle. Nonetheless, the fidelity of the navigation system is sufficient for targeting larger anatomic targets such as the ventricles, or pathology such as a hematoma, and could potentially be applied to navigation towards MRI defined targets with similar accuracy.[11,13] This system could be applied to intracranial access in either a hybrid operating room or an interventional angiographic suite with appropriate safety precautions. Burr holes have been performed in diagnostic MRI suites located in radiology for over a decade with complication rates that are comparable to the operating room setting.[26,27] FDCT and targeting could be performed following standard burr hole creation as with these experiments or potentially before if a safe location for a burr hole creation is considered in targeting.

The concept of FDCT procedural guidance has been successfully applied with slight variations to percutaneous procedures in the brain, head and neck, and spine.[1–3,7,8,10,11,14–16] There are some notable advantages to using FDCT guidance as opposed to conventional CT including potentially lower radiation doses depending on individual procedure specifics and the fact that a traditional CT room stays functional for diagnostic studies.[4,28,29] The radiation

metrics that we encountered in our study were within expected ranges of most interventional procedures and less than many angiographic procedures.[43031] For our procedures, the operator was only in the room for a small amount of fluoroscopy (mean 0.16 minutes) in order to shim the table into position and the operator's hand never entered the fluoroscopy beam. The second FDCT was performed as a second error measurement and could potentially be omitted in clinical practice depending on the need for needle confirmation. One notable difference between our technique and similar procedures described in the literature is that we did not advance the needle under fluoroscopic guidance, skipping any progression views (similar to Figure 2D) and instead only using the system's laser to line up the needle and advancing the needle in a single pass.[13112832] The progression view could potentially be useful as a guide for depth if needed. The radial error in our system could potentially be due to slight fusion mis-registration, mis-angulation in freehand targeting, or slight needle curvature along the course of its path. Our freehand technique likely contributed the most to error with slight mis-angulation expected and needle guidance devices could be explored in the future with our DBS phantom in order to potentially reduce error.[32] In order to continuously use the laser guidance system as the needle was passed, the operator had to stand to the side of the detector and head phantom with his hand controlling the needle between the detector and head phantom, this somewhat awkward positioning relative to standing directly over the patient could have also introduced some error to the technique with slight mis-angulation. Needle curvature is unlikely to have played a major role in error, as the phantom brain was all one consistency.

There are several limitations to consider in our study. Our study includes a relatively small number of needle passes and individual experiments across three sessions. The same head phantom was used for all and needle passes and the MRI was not repeated for each needle pass, however all fusion steps and the FDCT were repeated for each for each needle pass in order to be able to include any variation in fusion in our error assessment. Two-dimensional radial error was used as our measurement of accuracy as depth error was necessarily artificial due to the needle physically hitting the target. Depth could potentially be addressed in the future by incorporating a lateral progression view.

In conclusion, navigational guidance for single pass needle placement in the interventional suite using FDCT with or without fusion to pre-procedural MRI is associated with a radial error of approximately 2.5–3.0 mm at a depth of approximately 80 mm and acceptable radiation to the patient and operator. This system with free-hand, single-pass technique and with or without MRI fusion can be used to accurately target sub-centimeter intracranial lesions including those defined on MRI and provide guidance for spinal and head and neck procedures in the interventional angiographic suite or a hybrid operating room.

Acknowledgments

Funding Statement:

This work was supported by the US Department of Health and Human Services-National Institutes of Health (NIH) grant number NIH 5T32EB001631-10.

References

1. Yang Z, Hong B, Jia Z, et al. Treatment of supratentorial spontaneous intracerebral hemorrhage using image-guided minimally invasive surgery: Initial experiences of a flat detector CT-based puncture planning and navigation system in the angiographic suite. AJNR Am J Neuroradiol. 2014; 35(11):2170–5. [PubMed: 24994826]
2. Cooke DL, Levitt M, Kim LJ, et al. Intraorbital access using fluoroscopic flat panel detector CT navigation and three-dimensional MRI overlay. J NeuroIntervent Surg. 2010; 2:249–51.
3. Fiorella D, Peeling L, Denice CM, et al. Integrated flat detector CT and live fluoroscopic-guided external ventricular drain placement within the neuroangiography suite. J Neurointerv Surg. 2014; 6(6):457–60. [PubMed: 23892444]
4. Daly M, Siewerdsen J, Moseley D, et al. Intraoperative cone-beam CT for guidance of head and neck surgery: Assessment of dose and image quality using a C-arm prototype. Med Phys. 2006; 33(10):3767–80. [PubMed: 17089842]
5. Doelken M, Struffert T, Richter G, et al. Flat-panel detector volumetric CT for visualization of subarachnoid hemorrhage and ventricles: preliminary results compared to conventional CT. Neuroradiology. 2008; 50(6):517–23. [PubMed: 18330518]
6. Heran N, Song J, Namba K, et al. The utility of DynaCT in neuroendovascular procedures. AJNR Am J Neuroradiol. 2006; 27(2):330–2. [PubMed: 16484404]
7. Tam A, Mohamed A, Pfister M, et al. C-arm cone beam computed tomography needle path overlay for fluoroscopic guided vertebroplasty. Spine (Phila Pa 1976). 2010; 35(10):1095–9. [PubMed: 20139803]
8. Racadio J, Babic D, Homan R, et al. Live 3D guidance in the interventional radiology suite. AJR Am J Roentgenol. 2007; 189(6):W357–64. [PubMed: 18029850]
9. Söderman M, Babic D, Holmin S, et al. Brain imaging with a flat detector C-arm: Technique and clinical interest of XperCT. Neuroradiology. 2008; 50(10):863–8. [PubMed: 18560818]
10. Nesbit GM, Nesbit EG, Hamilton BE. Integrated cone-beam CT and fluoroscopic navigation in treatment of head and neck vascular malformations and tumors. J Neurointerv Surg. 2011; 3(2): 186–90. [PubMed: 21990816]
11. Cooke DL, Levitt M, Kim LJ, et al. Transcranial access using fluoroscopic flat panel detector CT navigation. AJNR Am J Neuroradiol. 2011; 32(4):E69–70. [PubMed: 20299429]
12. Struffert T, Richter G, Engelhorn T, et al. Visualisation of intracerebral haemorrhage with flat-detector CT compared to multislice CT: results in 44 cases. Eur Radiol. 2009; 19(3):619–25. [PubMed: 18813932]
13. Siewerdsen JH, Moseley DJ, Burch S, et al. Volume CT with a flat-panel detector on a mobile, isocentric C-arm: pre-clinical investigation in guidance of minimally invasive surgery. Med Phys. 2005; 32(1):241–54. [PubMed: 15719975]
14. Spelle L, Ruijters D, Babic D, et al. First clinical experience in applying XperGuide in embolization of jugular paragangliomas by direct intratumoral puncture. Int J Comput Assist Radiol Surg. 2009; 4(6):527–33. [PubMed: 20033329]
15. Nett B, Aagaard-Kienitz B, Serarslan Y, et al. A simple technique for interventional tool placement combining fluoroscopy with interventional computed tomography on a C-arm system. Neurosurgery. 2010; 67(3 Suppl Operative):49–56. discussion 56–7. [PubMed: 20559091]
16. Levitt MR, Vaidya SS, Su DK, et al. The “triple-overlay” technique for percutaneous diagnosis and treatment of lesions of the head and neck: combined three-dimensional guidance with magnetic resonance imaging, cone-beam computed tomography, and fluoroscopy. World Neurosurg. 2013; 79(3–4):509–14. [PubMed: 22484075]
17. Brommeland T, Hennig R. A new procedure for frameless computer navigated stereotaxy. Acta Neurochir (Wien). 2000; 142(4):443–7. discussion 47–8. [PubMed: 10883342]
18. Brommeland T, Hennig R. Mechanical accuracy of a new stereotactic guide. Acta Neurochir (Wien). 2000; 142(4):449–54. [PubMed: 10883343]
19. Kim IS, Son BC, Lee SW, et al. Comparison of frame-based and frameless stereotactic hematoma puncture and subsequent fibrinolytic therapy for the treatment of supratentorial deep seated

spontaneous intracerebral hemorrhage. Minim Invasive Neurosurg. 2007; 50(2):86–90. [PubMed: 17674294]

20. Paleologos TS, Dorward NL, Wadley JP, et al. Clinical validation of true frameless stereotactic biopsy: analysis of the first 125 consecutive cases. Neurosurgery. 2001; 49(4):830–5. discussion 35–7. [PubMed: 11564243]
21. Quinones-Hinojosa A, Ware ML, Sanai N, et al. Assessment of image guided accuracy in a skull model: comparison of frameless stereotaxy techniques vs. frame-based localization. J Neurooncol. 2006; 76(1):65–70. [PubMed: 16132501]
22. Widmann G, Eisner W, Kovacs P, et al. Accuracy and clinical use of a novel aiming device for frameless stereotactic brain biopsy. Minim Invasive Neurosurg. 2008; 51(6):361–9. [PubMed: 19061150]
23. Ringel F, Ingerl D, Ott S, et al. VarioGuide: a new frameless image-guided stereotactic system–accuracy study and clinical assessment. Neurosurgery. 2009; 64(5 Suppl 2):365–71. discussion 71–3. [PubMed: 19404116]
24. Martin AJ, Larson PS, Ostrem JL, et al. Placement of deep brain stimulator electrodes using real-time high-field interventional magnetic resonance imaging. Magn Reson Med. 2005; 54(5):1107–14. [PubMed: 16206144]
25. Larson PS, Starr PA, Bates G, et al. An optimized system for interventional magnetic resonance imaging-guided stereotactic surgery: preliminary evaluation of targeting accuracy. Neurosurgery. 2012; 70(1 Suppl Operative):95–103. discussion 03. [PubMed: 21796000]
26. Starr PA, Martin AJ, Ostrem JL, et al. Subthalamic nucleus deep brain stimulator placement using high-field interventional magnetic resonance imaging and a skull-mounted aiming device: technique and application accuracy. J Neurosurg. 2010; 112(3):479–90. [PubMed: 19681683]
27. Ostrem JL, Galifianakis NB, Markun LC, et al. Clinical outcomes of PD patients having bilateral STN DBS using high-field interventional MR-imaging for lead placement. Clin Neurol Neurosurg. 2013; 115(6):708–12. [PubMed: 22944465]
28. Braak SJ, van Strijen MJ, van Es HW, et al. Effective dose during needle interventions: cone-beam CT guidance compared with conventional CT guidance. J Vasc Interv Radiol. 2011; 22(4):455–61. [PubMed: 21463755]
29. Miracle AC, Mukherji SK. Conebeam CT of the head and neck, part 1: physical principles. AJNR Am J Neuroradiol. 2009; 30(6):1088–95. [PubMed: 19439484]
30. Kemerink GJ, Frantzen MJ, Oei K, et al. Patient and occupational dose in neurointerventional procedures. Neuroradiology. 2002; 44(6):522–8. [PubMed: 12070727]
31. Buls N, Pages J, de Mey J, et al. Evaluation of patient and staff doses during various CT fluoroscopy guided interventions. Health physics. 2003; 85(2):165–73. [PubMed: 12938963]
32. Kroes MW, Busser WM, Futterer JJ, et al. Assessment of needle guidance devices for their potential to reduce fluoroscopy time and operator hand dose during C-arm cone-beam computed tomography-guided needle interventions. J Vasc Interv Radiol. 2013; 24(6):901–6. [PubMed: 23602061]

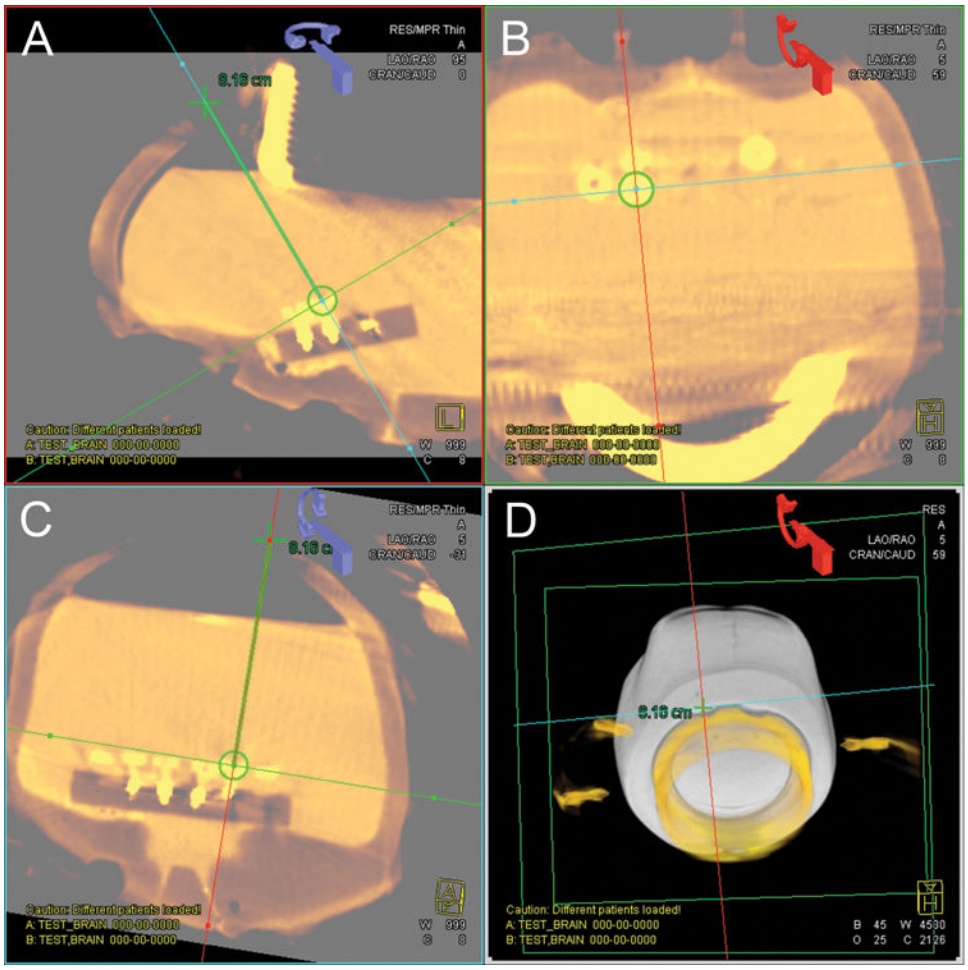

Figure 1.

Target selection on FDCT navigational software. In this step the FDCT data sets and the pre-procedural MRI data sets have been automatically fused and both displayed. The target was selected when windowed to the MRI data set and the entry site was selected when windowed to the FDCT data set. Sagittal (A), axial (B), and coronal (C) images are displayed for targeting as well as a path projection view (D).

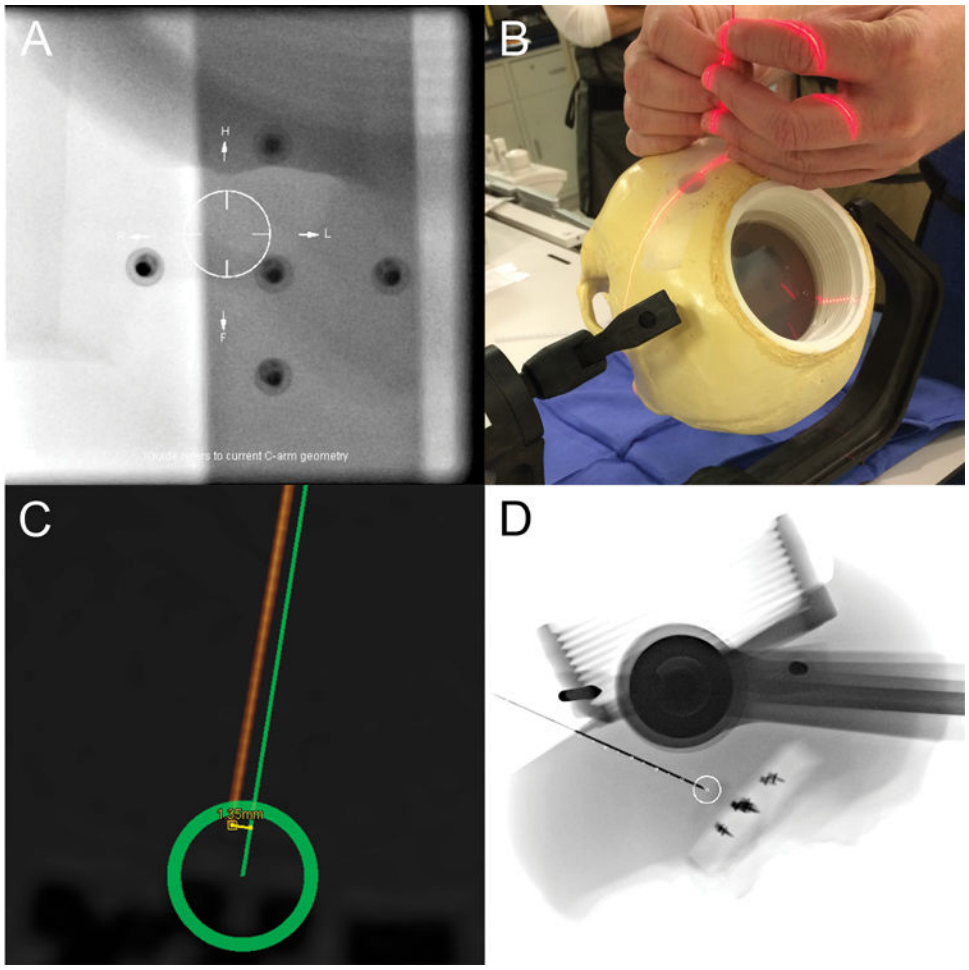

Figure 2.

Procedure and FDCT Error Measurement (A) Manual table shimming. Using the maximum fluoroscopic magnification setting (11 cm field of view) as depicted here and while fluoroscopy was off, the table was manually shimmed to line up the projected target and entry site by lining up the inner circle and crosshairs in the center of the four outer arrows. The underlying image is ignored as it does not represent the current position while shimming but rather the last fluoroscopy image. (B) Single pass needle placement. With fluoroscopy off the needle hub was aligned with the laser crosshair and the needle was advanced in a single pass until the target was reached. (C) and (D) Post-procedure FDCT. Radial error as measured by FDCT (C) from the needle tip to the planned needle trajectory/target. The green circle is a 10 mm sphere centered at the target. A lateral projection view (D) from the FDCT shows the needle in relationship to the planned needle trajectory. This is similar to a progression view that can be obtained during needle placement but was skipped during our procedures.

Figure 3.

Visual assessment of radial error. Through the large posterior hole in the phantom the target and concentric rings on the target could be visualized. A radial error measurement to the center point of the target was given for each needle placement. Each target is 10 mm in diameter and has an inner 3 mm diameter notch. The target is marked with 1mm concentric rings to allow visual assessment of radial error.

Table 1

Results of Single Pass Needle Placement and Radiation Output. The operator was not in the room for either FDCT. In practice the second FDCT could potentially be omitted.

Depth and Radial Error of FDCT Navigation for Single Pass Needle Placement				
Variable	**All (N=20)**	**MRI Fusion (N=10)**	**FDCT Only (N=10)**	**Two-tailed p**
Mean Depth	83.12 mm (SD 2.06)	83.08 mm (SD 1.72)	83.15 mm (SD 2.45)	0.968 (NS)
Mean visual radial error to center point	2.75 mm (SD 1.39)	2.55 mm (SD 1.09)	2.95 mm (SD 1.67)	0.596 (NS)
Mean radial error by FDCT	2.80 mm (SD 1.43)	2.60 mm (SD 1.05)	3.00 mm (SD 1.77)	0.675(NS)
Radiation Output				
	Mean Air Kerma (mGy)		Mean Dose Area Product (uGy-m^2)	Mean Fluoroscopy Time (minutes)
First FDCT for Targeting	60.39 (SD 6.81)		1624.88 (SD 183.26)	NA
Fluoroscopy for Lining up Target	1.21 (SD 1.89)		17.28 (SD 17.88)	0.16 (SD 0.14)
Second FDCT for Error Measurement	60.58 (SD 6.76)		1629.84 (SD 181.73)	NA
Total	122.19 (SD 12.95)		3272.00 (SD 327.74)	0.16 (SD 0.14)

SD=standard deviation, FDCT=flat panel detector computed tomography, MRI=magnetic resonance imaging, N=number, NS=non significant, NA=Not Applicable, mGy=milligray, uGy=microgray.